Wiley Online Library
Early View publication on www.wileyonlinelibrary.com
(issue and page numbers not yet assigned;
citable using Digital Object Identifier – **DOI**)

Phys. Status Solidi B, 1–5 (2014) / **DOI** 10.1002/pssb.201400040

physica status solidi b
www.pss-b.com
basic solid state physics

Charge transition level of GeP_{b1} centers at interfaces of $SiO_2/Ge_xSi_{1-x}/SiO_2$ heterostructures investigated by positron annihilation spectroscopy

O. Madia*[,1], N. Segercrantz[2], V. Afanas'ev[1], A. Stesmans[1], L. Souriau[3], J. Slotte[2], and F. Tuomisto[2]

[1] Department of Physics and Astronomy, University of Leuven, Celestijnenlaan 200D, Leuven 3001, Belgium
[2] Department of Applied Physics, Aalto University, P. O. Box 11100, Aalto 00076, Finland
[3] IMEC, Kapeldreef 75, Leuven 3001, Belgium

Received 29 April 2014, revised 9 August 2014, accepted 12 August 2014
Published online 25 September 2014

Keywords defects, electrical characterization, ESR, positron annihilation, semiconductor/oxide interface, SiGe

* Corresponding author: e-mail oreste.madia@fys.kuleuven.be, Phone: +32 476097872, Fax: +32 16 327987

In this work, we address the charge trapping properties of Ge dangling bond (DB) defects – GeP_{b1} centers as typified by electron spin resonance spectroscopy (ESR) – found at the interfaces between condensation-grown $Si_{1-x}Ge_x$ ($0.28 < x < 0.8$) alloys and insulating SiO_2. The ESR observation of singly-occupied paramagnetic GeP_{b1} centers, carried out at 4.3 K, is complemented by temperature-dependent positron annihilation spectroscopy (PAS) in the Doppler broadening mode, which enables observation of the neutral-to-negative defect transitions as the temperature increases from 50 to 300 K. Through correlation of this re-charging behavior with the temperature-induced shift of the Fermi energy, the energy of the Ge DB −/0 transition in the $Si_{0.27}Ge_{0.73}$ alloy is inferred to be energetically distributed in a ~0.1 eV interval above the top of the semiconductor valence band. This result refines previous estimates from capacitance–voltage measurements, thus providing independent affirmation that the energy levels of Ge DBs lie inside the band gap of the $Si_{1-x}Ge_x$ alloys.

1 Introduction Following the introduction of high-dielectric constant insulators and metallic gates, further improvement of metal–oxide–semiconductor (MOS) devices performance requires transition from silicon as channel material to high-mobility alternatives, such as germanium and silicon–germanium alloys. However, the Ge MOS technology still faces difficulties related to the high density of electron traps found near or at the semiconductor/insulator interface, which impair the device performance. The identification of these defects and evaluation of the defect energy level is therefore required to correctly estimate their impact on the MOS transistor operation.

Whereas it is well known that interface traps in Si/SiO_2 systems are mainly associated with dangling bonds (DBs) of Si atoms [1, 2], the manifestation of Ge DBs at Ge/oxide interfaces has so far been evasive because of the lack of a clear correlation between the observed electron traps and paramagnetic defects revealed by electron spin resonance (ESR), more specifically, no Ge DB related interface defects could be resolved [3]. In attempt to explain this discrepancy, it was proposed that DBs of Ge do not give rise to energy levels in the semiconductor band gap, but in the energy range corresponding to the Ge valence band (VB) [4]. This would make them always doubly occupied (negatively charged) and, therefore, diamagnetic. Recently, Ge DBs were claimed to be found by using electrically detected spin resonance in oxidized Ge [5], though no estimate of their density is reported. On the other hand, the classical absorption-detection ESR has successfully characterized and quantified Ge DB centers in condensation grown Ge_xSi_{1-x}/SiO_2 ($0.28 \leq x \leq 0.8$) heterostructures [6]. Using the correlation with electrical results obtained on the same samples, the observed defects, typified as Ge P_{b1} centers, were found to behave as shallow acceptors [7]. This conclusion raises a fundamental question regarding their atomic nature and charged state because the "classical" DBs, such as the well-known Si P_b-type centers, are paramagnetic when in the singly occupied (neutral) state, while the doubly occupied

(negative) centers are diamagnetic. In preliminary work [6], we have independently confirmed the presence of a negative charge associated with unpassivated defect, using positron annihilation spectroscopy (PAS) experiments. Here, by further exploring the temperature dependences of the PAS response, we have found that there is a correlation between the ESR and positron signals coming from the negatively charged defects in as-grown and passivated structures.

2 Experimental The $(100)Si/SiO_2/Ge_xSi_{1-x}/SiO_2$ heterostructures studied in this work have been prepared by the condensation growth method on a 200 mm diameter SOI wafer with 22 nm thick boron doped ($N_a \approx 5 \times 10^{17}\,cm^{-3}$) top Si layer and a 140 nm-thick buried oxide (BOX) layer. First, a Si-rich Ge_xSi_{1-x} ($x = 0.24$–0.27) layer was epitaxially grown on the SOI wafer using SiH_4 and GeH_4 as precursors in an ASM Epsilon®2000 reactor, which was followed by the growth of a thin (7 nm) epi-Si layer on top to prevent out diffusion of Ge during the initial stage of thermal oxidation. Next, selective thermal oxidation of Si atoms is carried out in pure oxygen. By choosing the process temperatures above the thermal stability limit of Ge oxide, one is able to exploit two concomitant phenomena: selective oxidation of Si into SiO_2 at the top interface, and diffusion of Ge atoms through the GeSi and the Si layer of the SOI. Piling-up of Ge at the oxidizing top interface is therefore prevented, thus leading to a gradual homogeneous Ge enrichment of the initial Ge_xSi_{1-x} layer. In total, three steps of dry oxidation (at 1150, 1000, and 900 °C) were performed, each followed by annealing in inert (Ar) ambient. Cross-sectional TEM images of the heterostructures and additional details regarding the fabrication technique can be found elsewhere [7–9]. Passivation of defects was carried out by heating the samples in H_2 (99.9999%) at 1.05 atm for 35 ± 1 min at 450 °C as reported in Ref. [10].

To assess the charge state of the Ge DBs, we used the PAS in the Doppler broadening mode. These experiments were conducted using a monoenergetic positron beam emitted by a ^{22}Na source and moderated by a W foil. The annihilation γ-rays (photon energy $E_\gamma = 511$ keV) were detected using a high-purity Ge detector with energy resolution of 1.3 at 511 keV. The line shape parameters S, W are defined as the fraction of counts in the central window (S) and in the wings (W) of the annihilation peak with respect to the total number of counts. The symmetric S energy window was typically chosen in the range $|E_\gamma - 511\,\text{keV}| < 0.83$ keV around the peak of the energy distribution of the annihilation photons E_γ. The W parameter was evaluated from the wings of the annihilation photon distribution symmetrically in the range $3.00\,\text{keV} < |E_\gamma - 511\,\text{keV}| < 7.60$ keV. After being implanted in the sample under investigation, positrons require a few picoseconds to thermalize. Then, after diffusion for tens to hundreds of nanometers depending on material density, they ultimately annihilate with electrons producing two photons with energy of about 511 keV. Since the (non-zero) momentum of the electron–positron pair is conserved in the annihilation event, there is an additional energy contribution which broadens the 511 keV photon energy line. This effect can be quantified by using the line shape parameters S and W, also referred to as low and high momentum parameters, defined as the ratio between the events detected in the central window (S) and wings (W) of the annihilation peak, with respect to the total number of counts. The measured S and W parameters reflect superposition of different components, each one associated with a characteristic positron state inside the sample under investigation. In the presence of only two positron trapping states (e.g., at the surface and in the bulk), the measured S and W parameters can be expressed as linear combinations of the surface and bulk contributions:

$$\begin{aligned} S_{\text{measured}} &= A_S S_{\text{surface}} + B_S S_{\text{bulk}}, \\ W_{\text{measured}} &= A_W W_{\text{surface}} + B_W W_{\text{bulk}}. \end{aligned} \tag{1}$$

With increasing positron acceleration energy, one will find the S, W values to evolve along a straight line connecting the two characteristic states in the (S, W) plane. Would a nonlinear behavior be observed in this S versus W plot, it will then indicate the presence of additional annihilation states. The latter appears to be not the case in the S, W range shown in Fig. 1. More details on the PAS technique and its experimental realization can be found elsewhere [11–13].

3 Results The ESR experiments are limited to probing of defects in the paramagnetic state, such as singly occupied DBs (generally in the neutral state). As reported in Ref. [6, 7], the coexistence between ESR active Ge P_{b1} centers at the Ge_xSi_{1-x}/SiO_2 interface and an equal amount of shallow acceptor traps as found from electrical results obtained at 300 and 77 K, needs some explanation. From PAS experiments performed at room temperature we found that the defects present at the interface between Ge_xSi_{1-x} and SiO_2 also constitute an efficient trapping site for positrons [6].

ESR spectroscopy and electrical characterization are consistent in revealing that the samples containing 73 and 75% of Ge in the Ge_xSi_{1-x} layer exhibit the highest amount of Ge P_{b1} interfacial defects [7]. The (S, W) plots obtained on these samples, shown in Fig. 1, clearly show a clustering of points, indicating the presence of a positron trapping site. This result is further corroborated by the analysis of the S parameter as a function of positron acceleration energy (not shown here), where the occurrence of a plateau in the S parameter also points to the presence of a positron trapping site associated with Ge_xSi_{1-x} layer. Figure 2a shows the S versus E_a curves, where E_a represents the positron acceleration energy for the unpassivated (H-free) sample containing 73% of Ge in the Ge_xSi_{1-x} layer. As the measurement temperature is lowered from 300 to 50 K a clear shift of the S value is observed. Importantly, the change in the S parameter at $E_a = 1$ and 2 keV does not follow the changes at the surface (measurement points at 0.3 keV) where, regarding the latter, after the initial drop when decreasing the temperature from 300 to 200 K, there is hardly any change occurring for further lowering of the

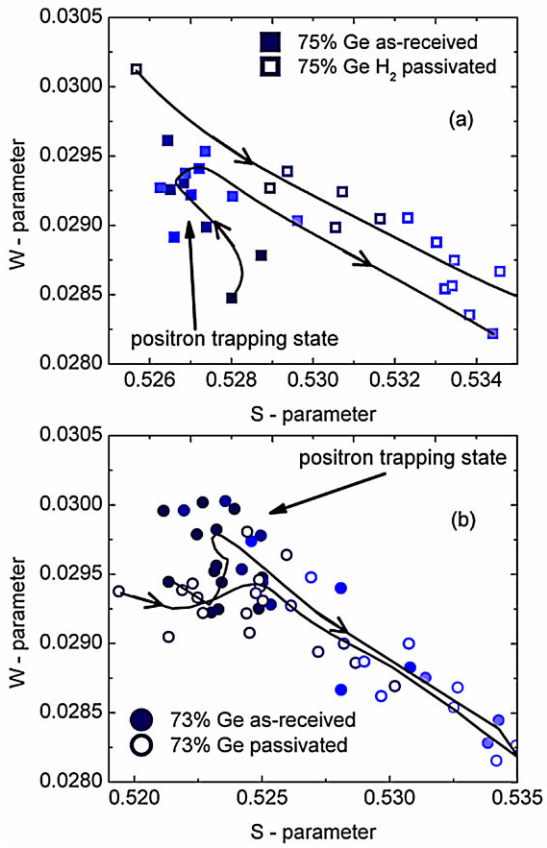

Figure 1 The line shape parameters (S, W) measured in the studied (100)Si/SiO_2/Ge_xSi_{1-x}/SiO_2 entities containing 75% Ge (a) and 73% Ge (b), before (filled symbols) and after (empty symbols) passivation of interface defects by H_2. The solid curves with arrow indicate increasing positron acceleration energies.

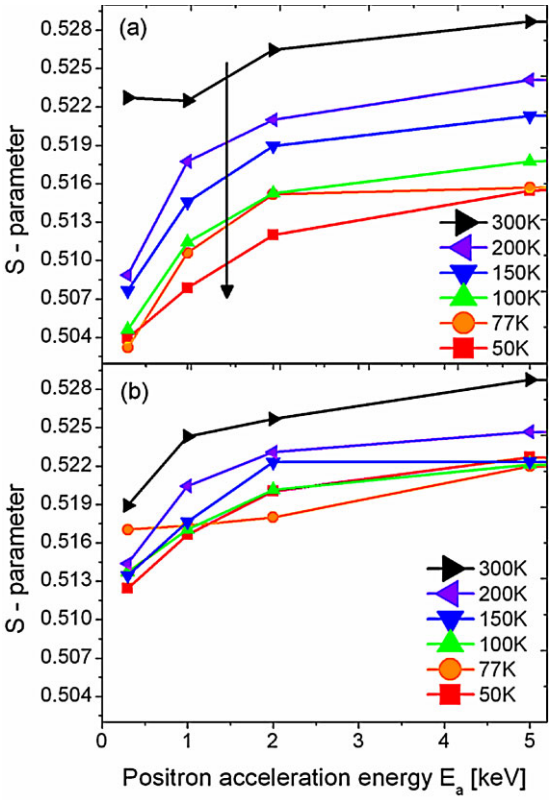

Figure 2 S-parameter, as a function of positron implantation energy, measured at different temperatures in the (100)Si/SiO_2/$Ge_{0.73}Si_{0.27}$/SiO_2 sample in the as-received state (a) and after passivation in H_2 (b).

observational temperature. This suggests that (i) positrons do not diffuse efficiently to the surface, pointing to the presence of an important concentration of positron traps and (ii) there is negative charge associated with these traps as otherwise no or very little temperature effect should be observed. Finally, the S versus E_a becomes gradually flatter when the temperature is reduced from 200 to 50 K. This suggests that the effect of positron trapping within the materials becomes less important at the lowest temperatures.

As the data shown in Fig. 2b suggest, this temperature effect is strongly reduced for the sample passivated by annealing in hydrogen, resulting in more homogeneously distributed S parameter for all acceleration energies. This change in the behavior reflects a strongly reduced contribution of the positron annihilation states related to the traps at the Ge_xSi_{1-x}/SiO_2 interfaces. The relative variation of the S parameter evaluated at low acceleration energies (1 and 2 keV) as a function of sample temperature is presented in Fig. 3. The data from the unpassivated sample (filled squares and circles) exhibit a substantial linear increase with temperature and the corresponding relative increase of the S parameter reach ~3% when increasing the temperature from 50 to 300 K. On the contrary, the measurements repeated after hydrogen passivation (filled triangles) exhibit a much weaker temperature dependence. Interestingly, a similar weak increase of the S value can be

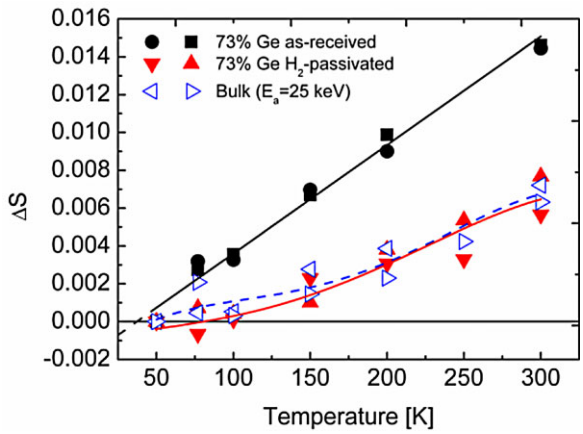

Figure 3 Relative variation of S-parameter, evaluated at low positron implantation energies ($E_a = 1$ and 2 keV) as a function of measurement temperature in the (100)Si/SiO_2/$Ge_{0.73}Si_{0.27}$/SiO_2 sample prior (black circles and squares) and after (red filled triangles) passivation in H_2. Measurements for high implantation energy (open triangles) are included for comparison.

seen in the results obtained on both samples (i.e., prior and after the passivation of defects by hydrogen) when the acceleration energy is sufficient to implant positrons deep into the Si substrate wafer (open triangles in Fig. 3). This would allow one to exclude the influence of additional temperature-related positron transport phenomena in the sample, indicating that the upward S value shift observed for the $E_a = 1$ keV and $E_a = 2$ keV measurements is predominantly associated with positron trapping found at the sites located at the first interface between Ge_xSi_{1-x} and SiO_2. Within the explored temperature range the structural stability of the samples is ensured and the number of interfacial DB defects is unaffected. Therefore, the temperature-induced effect is probably caused by the shift of the Fermi level, resulting in a change in the DB charge state. This trend has been previously demonstrated by observing the Grey-Brown shift of the 100 kHz capacitance–voltage curve on MOS structures fabricated by evaporation of aluminum contacts on top of the SiO_2 insulator. This shift is illustrated in Fig. 4 for the model case of the unpassivated sample with 55% Ge in the Ge_xSi_{1-x} layer. Regarding the sample used in this work, the amount of unpassivated charges did not allow us to reach depletion in the GeSi layer due to oxide breakdown. We therefore can correlate the PAS results to the change in occupancy of the DB defects, which occurs when the Fermi level in the Ge_xSi_{1-x} layer crosses the defect charge transition level. Since positron trapping arises from the interaction with the negative charge gained by a defect as the Fermi level shifts further away from the VB maximum, the interface-related contribution to the annihilation becomes more and more pronounced as temperature increases. This allows one to estimate the position of the defect charge transition level by evaluating the position of the Fermi energy (E_F) at different temperatures, as quantified by Eq. (2.20) in Ref. [14]. The intrinsic carrier concentration, n_i, has been calculated according to Ref. [15], while the hole concentration p has been estimated previously to be in the $(2–5) \times 10^{17}\,cm^{-3}$ range on the basis of Hall-effect and resistivity measurements [16]. Since this concentration of charge carriers is calculated assuming a uniform carrier distribution across the Ge_xSi_{1-x} layer thickness, it represents the *lower* limit of the hole concentration at the Ge_xSi_{1-x}/SiO_2 interface: The $C–V$ curves shown in Fig. 4 indicate that the p-type Ge_xSi_{1-x} surface is in the state of accumulation at zero external bias. Therefore, the calculated variation of the Fermi level position from ~0.11 to 0.01 eV above the VB top edge as the sample is cooled from 300 to 50 K, provides the *upper* limit of the energy location of the Ge P_{b1} centers above the Ge_xSi_{1-x} VB. The calculations indicate that the Fermi level position in the $Ge_{0.73}Si_{0.27}$ layer varies from a maximum value of 0.11 to 0.01 eV above the VB maximum as the sample is cooled down from 300 to 50 K. The charge transition levels of the Ge P_{b1} centers are thus inferred to lie within this energy range.

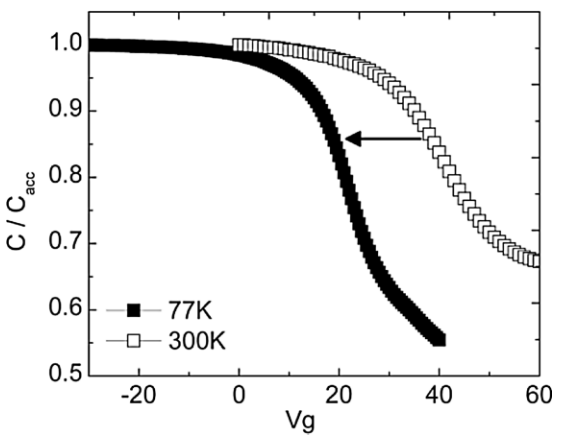

Figure 4 Temperature induced shift of 100 kHz ($C–V$) curve measured at 300 K (open squares) and 77 K (filled squares) in the sample containing 55% of Ge accordingly to Refs. [6, 7].

4 Conclusions The energy level of Ge DB defects, found at the interfaces of condensation-grown Ge_xSi_{1-x} layers with SiO_2 is inferred to lie in the Ge_xSi_{1-x} alloy band gap close to VB. Previous results revealed that these defects act as efficient trapping sites for positrons, allowing for meaningful characterization through PAS in Doppler broadening mode. The analysis of the S parameter value as a function of positron acceleration energy suggests enhanced post-thermalization diffusion of positrons towards the surface as the temperature becomes lower, which correlates with a reduced density of positron traps in the Ge_xSi_{1-x} layer.

As main conclusion, it is thus found that the positron trapping is associated with the negative charge trapped by the Ge P_{b1} defects as a consequence of the shift of the Fermi level within the semiconductor band gap. The corresponding defect charge transition from double (negatively charged) to single (neutral state) occupation is revealed in the explored temperature range (300–50 K) to be in the energy interval of ~0.1 eV near the $Ge_{0.73}Si_{0.27}$ VB top.

Acknowledgements This work has received financial support from the EU FP7 project MORDRED (Grant No. 261868) and COST European Cooperation in Science and Technology, action CM1104 "Reducible oxides."

References

[1] E. H. Poindexter, Semicond. Sci. Technol. **4**, 961–969 (1989).
[2] N. H. Thoan, K. Keunen, V. V. Afanas'ev, and A. Stesmans, J. Appl. Phys. **109**, 013710 (2011).
[3] V. V. Afanas'ev, Y. G. Fedorenko, and A. Stesmans, Appl. Phys. Lett. **87**, 032107 (2005).
[4] C. G. Van de Walle, M. Choi, J. R. Weber, J. L. Lyons, and A. Janotti, Microelectron. Eng. **109**, 211–215 (2013).
[5] M. Fanciulli, A. Molle, S. Baldovino, and A. Vellei, Microelectron. Eng. **88**(7), 1482–1487 (2011).
[6] O. Madia, A. P. D. Nguyen, N. H. Thoan, V. V. Afanas'ev, A. Stesmans, L. Souriau, J. Slotte, and F. Tuomisto, Appl. Surf. Sci. **291**, 11–15 (2014).
[7] V. V. Afanas'ev, M. Houssa, A. Stesmans, L. Souriau, R. Loo, and M. Meuris, Appl. Phys. Lett. **95**, 222106 (2009).

[8] L. Souriau, V. Terzieva, W. Vandervorst, F. Clemente, B. Brijs, A. Moussa, M. Meuris, R. Loo, and M. Caymax, Thin Solid Films **517**, 23–26 (2008).
[9] L. Souriau, T. Nguyen, E. Augendre, R. Loo, V. Terzieva, M. Caymax, S. Cristoloveanu, M. Meuris, and W. Vandervorst, J. Electrochem. Soc. **156**, H208 (2009).
[10] N. H. Thoan, A. Stesmans, A. P. D. Nguyen, K. Keunen, and V. V. Afanas'ev, J. Vac. Sci. Technol. B **31**, 010603 (2013).
[11] J. Slotte and F. Tuomisto, Mater. Sci. Semicond. Process. **15**, 669–674 (2012).
[12] F. Tuomisto and I. Makkonen, Rev. Mod. Phys. **85**, 1583 (2013).
[13] S. Kilpeläinen, J. Kujala, F. Tuomisto, J. Slotte, Y. W. Lu, and A. N. Larsen, J. Appl. Phys. **114**, 164316 (2013).
[14] E. H. Nicollian and J. R. Brews, MOS (Metal Oxide Semiconductor) Physics and Technology (John Wiley & Sons, Hoboken, NJ, 2003), pp. 30–54.
[15] F. Schäffler, in: Properties of Advanced Semiconductor Materials: GaN, AIN, InN, BN, SiC, SiGe, edited by M. E. Levinshtein, S. L. Rumyantsev, and M. S. Shur (John Wiley & Sons, New York, 2001), pp. 149–188.
[16] N. Hirashita, Y. Moriyama, S. Nakaharai, T. Irisawa, N. Sugiyama, and S. Takagi, Appl. Phys. Express **1**, 101401 (2008).